ISIJ International, Vol. 42 (2002), No. 1, pp. 71–79

Factors on the Measurement of Effective Thermal Diffusivity of Molten Slag Using Double Hot Thermocouple Technique

Yoshiaki KASHIWAYA and Kuniyoshi ISHII

Division of Materials Science and Engineering, Graduate School of Engineering, Hokkaido University, Sapporo 060-8628 Japan. E-mail: Yoshiaki@eng.hokudai.ac.jp

(*Received on June 21, 2001; accepted in final form on September 11, 2001*)

The molten slags that are used not only in the continuous caster but also in every metal industry play an important role and affect the quality of products. The authors initially developed the double hot thermocouple technique (DHTT) for *in situ* observation of mold slag crystallization.

In this study, the DHTT was further developed to allow the measurement of the overall thermal diffusivity of molten slag applying the principle of the laser flash method. The affecting factors (finite pulse time, shape of pulse and heat loss from sample surface) on the measurement of thermal diffusivity using the DHTT were discussed theoretically using both the analytical and the numerical methods. New relationship between the thermal diffusivity α and the time at half-maximum temperature $t_{0.5}$ was obtained as follows:

$$\alpha(\times 10^4\ \mathrm{m^2/s}) = 0.000707(t_{0.5}/t_p)^{-1.8946}$$

The thermal diffusivity obtained from the experimental half-maximum time $t_{0.5}/t_p$ (t_p is the time of peak on the heat pulse) was in good agreement with the one from literature.

KEY WORDS: thermal diffusivity; thermal conductivity; slag melt; laser flash; hot thermocouple; DHTT.

1. Introduction

The physicochemical and the thermal properties of molten slag have large influence on the quality of products not only in the continuous caster but also in every high temperature process using a slag-metal reaction. The former properties such as the viscosity and melting-solidifying behavior have been widely investigated. Although the thermal conductivity (or diffusivity) was also measured by many researchers, the interests might mainly be focused on the inherent value such as a phonon conduction to eliminate the effect of radiation and the effect of other phenomena (convection, crystallization and bubble formation). Scientifically it would be important, however, practically, the overall heat transfer that includes the complicated phenomena such as the bubble formation and the crystallization will be more important and useful. Under such a situation, the direct observation during measurement of the thermal diffusivity can be a key technique to understand the obtained results adequately. The authors initially have developed the double hot thermocouple technique (DHTT) for *in situ* observation of mold slag crystallization.[1,2] These studies have indicated that the overall heat transfer rate in the actual process must be very complicated due to the interaction of crystallization of slag with the primary mechanisms of heat transfer: radiation, conduction and convection. The DHTT has a superior feature on the rapid heating and cooling of melted sample during observation, whereas the extremely high sensitivity on the temperature change makes it unamenable. The measurement of thermal diffusivity using the DHTT should overcome the following problems belonging to two categories:

(i) contents of the effective thermal diffusivity (effects of phonon conduction, radiation conduction, electron conduction and effect of convection)

(ii) influences of the experimental setup on the measured value.

In the present study, we focused on the problem of the second category (ii). The problem of the first one (i) will be discussed in the following paper.

The final purpose of present project is to clarify the effective thermal diffusivity during the bubble formation and crystallization. In this study, the DHTT was further developed and the measurements of thermal diffusivity using the standard sample (B_2O_3) were carried out. The affecting factors (finite pulse-time effect(shape of pulse) and heat loss from sample surface) on the measurement using the DHTT were elucidated and new relationship between the thermal diffusivity α and the time at half-maximum temperature $t_{0.5}$ was obtained, which was the modified relationship of Parker's method.[3,4]

2. Experimental

The details of experimental apparatus have been shown in the previous study.[1,2] **Figure 1** illustrates the principle of the thermal diffusivity measurement and the comparison of the alignment of heat source and detector between the

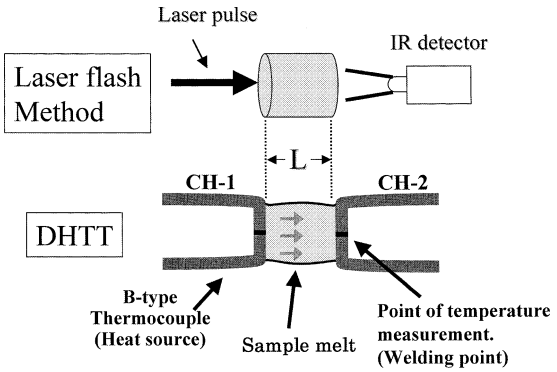

Fig. 1. Illustration of principle for the measurement of thermal diffusivity by DHTT (Double Hot Thermocouple Technique) comparing with the laser flash method.

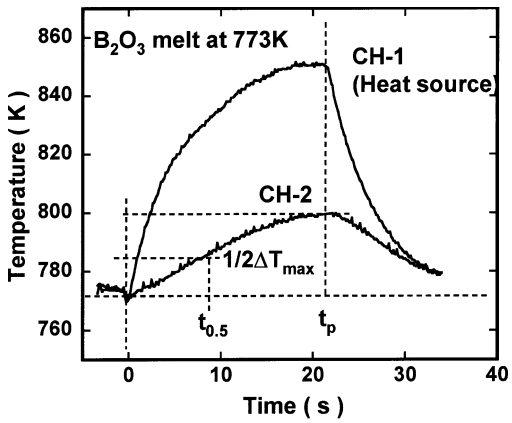

Fig. 2. Typical temperature profiles for measuring the thermal diffusivity.

DHTT and the laser flash method. The laser flash method is an excellent method and can predict a relatively suitable value of thermal diffusivity using Parker's method[4] (Eq. (3)). However, it will need a special alignment for the measurement of liquid and/or transparent material. Furthermore, a direct observation during measurement is almost impossible. On the other hand, the DHTT can observe the molten sample *in situ*. As shown in the previous study,[1,2] the solidification of mold slag is complicate phenomena including the bubble formation/breaking and the crystallization. It would be very important to know the sample image during measurement. The thermal diffusivity obtained from DHTT, however, is not yet established and it is not reported what kinds of factors affected on the measurement until now.

For the preliminary approach to the application of the DHTT to the measurement of thermal diffusivity, the affecting factors on the measurement were elucidated from both the theoretical and the experimental method. In the case of laser flash method, an instantaneous laser pulse was used as a heat source and the temperature increase at the rear surface was measured by an infrared pyrometer (IR detector). In the case of DHTT, the temperature of one side thermocouple (CH-1, in Fig. 1) increased in a pulse shape and the other side of thermocouple (CH-2) was used as a detector. The typical temperature profiles of both CH-1 and CH-2 are shown in **Fig. 2**. The time $t_{0.5}$ at the half-maximum temperature ($1/2\,\Delta T_{max}$) was defined as shown in Fig. 2 and used for the calculation of thermal diffusivity according to the laser flash method (the details will be shown in below). The large differences between the laser flash method and DHTT are as follows:

(1) Heat source is the order of several seconds (millisecond order in laser flash method).
(2) Shape of pulse is not square. This factor might be decisive in both the methods, however, the extent of delay on the pulse (finite pulse-time) is significant on the DHTT.
(3) Heat loss owing to the radiation and the conduction to the thermocouple (CH-2) for detection is significant for the DHTT.

In the present paper, these difficulties will be overcome for using the DHTT on the measurement of thermal diffusivity, because it can provide us with the other benefits such as the measurement of transparent slag melt and the direct observation. **Figure 3** shows the examples of the observations during measurements. Figure 3(a) is a sodium silicate melt ($Na_2O \cdot 2SiO_2$) having bubbles supported by the two thermocouples. On the other hand, Fig. 3(b) shows a clear and transparent B_2O_3 melt, in which many reflections could be seen because it was working as a lens. In this experiment, the bubbles were eliminated and clean melt was used.

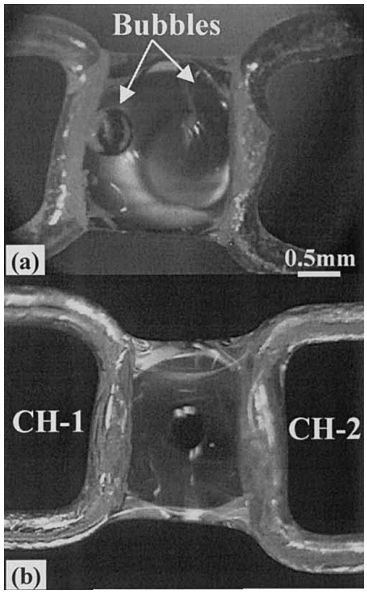

Fig. 3. Sample melts on the double hot thermocouple: (a) with bubbles ($Na_2O \cdot 2SiO_2$), (b) without bubble (B_2O_3). (Many reflections can be seen on the surface of sample, but sample itself is clear and transparent.)

3. Results and Discussions

The one dimensional heat transfer under an insulating condition with an instantaneous heat source was given by Carslaw and Jaeger.[3]

$$T(x,t)=\frac{1}{D}\int_0^D T(x,0)dx+\frac{2}{D}\sum_{n=1}^{\infty}\exp\left(\frac{-n^2\pi^2\alpha t}{D^2}\right)\times\cos\frac{n\pi x}{D}\int_0^D T(x,0)\cos\frac{n\pi x}{D}dx \quad \cdots\cdots\cdots\cdots(1)$$

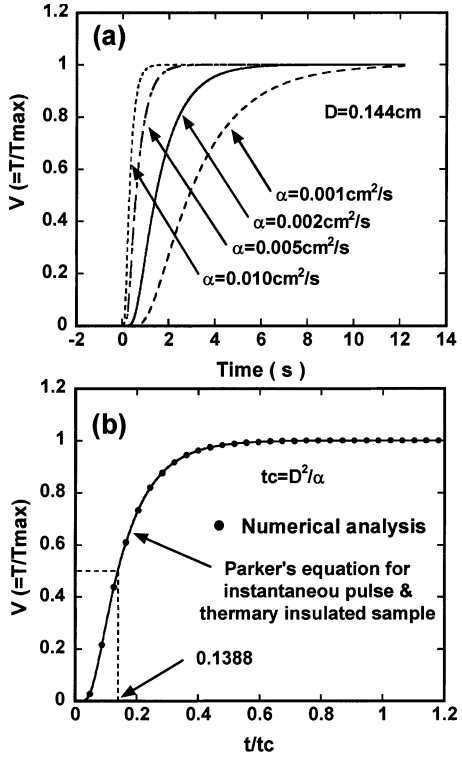

Fig. 4. Temperature profiles for different thermal diffusivities, which were calculated using Parker's equation for instantaneous pulse and thermally insulated sample.

where $T(x, 0)$ is the initial temperature distribution, $T(x, t)$ is the temperature distribution at any later time t and α is the thermal diffusivity. D means the thickness of sample. The temperature history V at the rear surface ($x=D$) can be expressed by Eq. (2).

$$V=\frac{T(D,t)}{T_M}=1+2\sum_{n=1}^{\infty}(-1)^n\times\exp\left(\frac{-n^2\pi^2}{D^2}\alpha t\right) \quad .....(2)$$

where T_M is the maximum temperature at the rear surface ($T_M=Q/\rho C_p D$, Q is the radiant energy of pulse, ρ is the density of sample and C_p is the heat capacity). From Eq. (2), Parker, *et al.*[4] gave the simplest equation expressed by Eq. (3). The time $t_{0.5}$ can be defined by that at $V=0.5$, which means the half-maximum temperature. Then, the thermal diffusivity α can be calculated by Eq. (3).

$$\alpha=0.1388\frac{D^2}{t_{0.5}} \quad .....(3)$$

Equation (3) is very useful equation to obtain the thermal diffusivity. Many commercial devices for measuring the thermal diffusivity have been developed on the basis of Eq. (3). **Figure 4** shows the temperature variations that calculated using Eq. (2) with different thermal diffusivities. Since the range of thermal diffusivity of slag melt is generally from 0.001×10^{-4} (m^2/s) to 0.02×10^{-4} (m^2/s), the time for reaching the maximum temperature is about from 2 to 10 sec depending on the thermal diffusivity. When we used the characteristic thermal diffusion time $t_c(=D^2/\alpha)$, those lines can be expressed with one line (Fig. 4(b)) and the relationship of Eq. (3) can be obtained for thermal diffusivity.

Since Eq. (3) was very convenient one to obtain the thermal diffusivity (otherwise whole temperature profile should be calculated for determining the thermal diffusivity), the meaning of Eq. (3) was analyzed. Then, the analogical and fundamental equation was derived as follows:

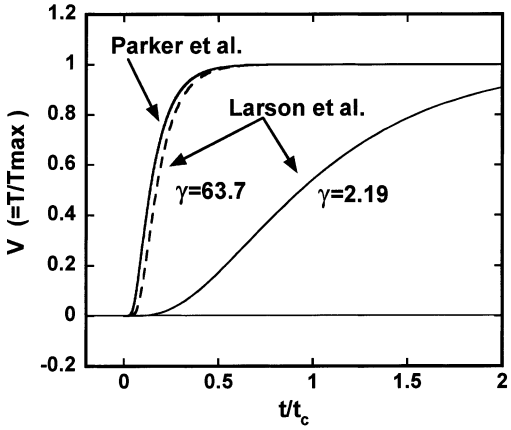

Fig. 5. Comparison of temperature profiles between different heat pulse using Parker's and Larson's equations.

$$\alpha=\vartheta_1\cdot t_{0.5}^{-\vartheta_2} \quad .....(4)$$

where ϑ_1 and ϑ_2 are the parameters determined by the sample thickness D, the heat loss and the finite pulse time (pulse shape). In the case of the instantaneous pulse and the insulated condition ($\vartheta_1=0.1388D^2$ and $\vartheta_2=1$), Eq. (4) is equal to Eq. (3) (Parker' equation). In the present study, the parameters, ϑ_1 and ϑ_2 were obtained for getting the adequate thermal diffusivity using DHTT.

3.1. Effect of Finite Pulse-time (Shape of Pulse)

Since the actual heat source is not instantaneous exactly (effect of finite pulse-time) and the heat loss cannot be avoided from the sample surface, several correction factors will be introduced more or less to obtain the correct value even in an actual commercial device, in which the thermal diffusivity is calculated based on the Eq. (3).

In such a circumstance, the effects of finite pulse-time have been studied by Larson *et al.*,[5] Taylor *et al.*[6] and Cape *et al.*[7] Larson *et al.* has applied the empirical exponential type pulse representing the output from xenon flash lamp on the theoretical analysis (Eq. (5)).

$$V=\frac{T(D,t)}{T_M}=1+2\gamma^2\sum_{n=1}^{\infty}(-1)^n\times\frac{\exp\left(\frac{-n^2\pi^2}{t_c}t\right)}{(\gamma-n^2\pi^2)^2}$$
$$-\gamma^{1/2}\frac{\exp\left(\frac{-t}{t_p}\right)}{2\sin\gamma^{1/2}}\left(1+2\frac{t}{t_p}+\gamma^{1/2}\cot\gamma^{1/2}\right) \quad .....(5)$$

where t_p is a time at peak of heat source pulse, γ is defined as t_c/t_p. In Eq. (5), the heat source was expressed as $\phi(t/t_c)=\gamma(t/t_c)\exp[(1-\gamma(t/t_c)]$. When $\gamma\to\infty$, Eq. (5) is equal to Eq. (2) for the instantaneous pulse by Parker *et al.* (Fig. 5) and the small value of γ means the delayed pulse. In **Fig. 5**, the two cases of calculation results for $\gamma=2.19$ and $\gamma=63.7$ are shown in comparison with that of Parker *et al.* It could be seen that the delayed pulse gave the inadequate

thermal diffusivity significantly, if the Eq. (3) was used.

From Larson's results, it was found that the effect of pulse shape (finite pulse-time) was important and the error for the thermal diffusivity sometime became several times.

3.2. Effect of Heat Loss

In addition to the effect of pulse shape, the heat loss from sample surface is quite important. Especially in the DHTT, the heat loss from the sample surface is relatively large and the conduction to the thermocouple for the detection (CH-2) is considerably large comparing to the radiation loss. Watt[8] has shown the theoretical approach for the radiation loss from the sample surface based on the equation by Carslaw *et al.*[3] Heckman[9] has studied the finite pulse-time effect and the heat loss using Green's function based on the result of Watt. For the triangular heat pulse (Fig. 6), Heckman has presented the relationship shown as Eq. (6).

$$V=\frac{T(D,t)}{T_\infty}=2\sum_{n=1}^{\infty}Y_n(0)Y_n(D)\left[M_n(t)+N_n\exp\left(\frac{-\beta_n^2 t}{t_c}\right)\right] \quad \text{.....(6)}$$

where

$$Y_n(x)=\frac{2^{1/2}(\beta_n^2+L_2^2)^2[\beta_n\cos(\beta_n x/D)+L_1\sin(\beta_n x/D)]}{[(\beta_n^2+L_1^2)(\beta_n^2+L_2^2+L_2)+L_1(\beta_n^2+L_2^2)]^{1/2}} \quad \text{.....(7)}$$

and the $\beta_n (n=1, 2, 3\ldots.)$ are the positive roots of the following equation (some numerical solutions are given in Appendix I).

$$(\beta_n^2-L_1L_2)\tan\beta_n=\beta_n(L_1+L_2) \quad \text{.....(8)}$$

where L_1 and L_2 mean the heat loss by radiation at the front and rear surface, respectively, and expressed by Eq. (9).[8]

$$L_m=D\frac{4\sigma\varepsilon T_m^3}{\kappa} \qquad (m=1 \text{ or } 2) \quad \text{.....(9)}$$

where σ is the Stefan–Boltzmann constant, ε is the emissivity of the sample surface, κ is the thermal conductivity and T_m is the temperature.

M_n and N_n in Eq. (6) are expressed as follows;

for $b\tau \leqq t \leqq \tau$,

$$M_n(t)=\frac{(B_n-B_n\cdot t/\tau+B_n^2)}{(1-b)} \quad \text{.....(10)}$$

$$N_n=\frac{B_n^2}{b}-\frac{B_n^2}{b(1-b)}\exp\left(\frac{b}{B_n}\right) \quad \text{.....(11)}$$

for $t>\tau$,

$$M_n(t)=0 \quad \text{.....(12)}$$

$$N_n=B_n^2\left(\frac{1}{b}+\frac{\exp(1/B_n)}{1-b}-\frac{\exp(b/B_n)}{b(1-b)}\right) \quad \text{.....(13)}$$

where

$$B_n=\frac{t_c}{\tau\beta_n^2} \quad \text{.....(14)}$$

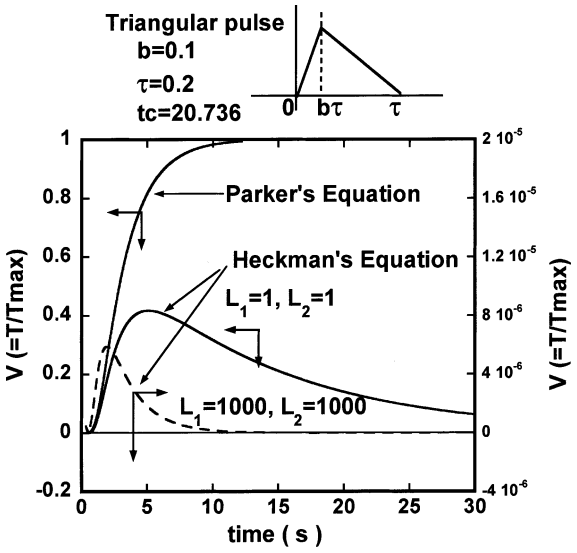

Fig. 6. Effect of heat loss on the temperature profile.

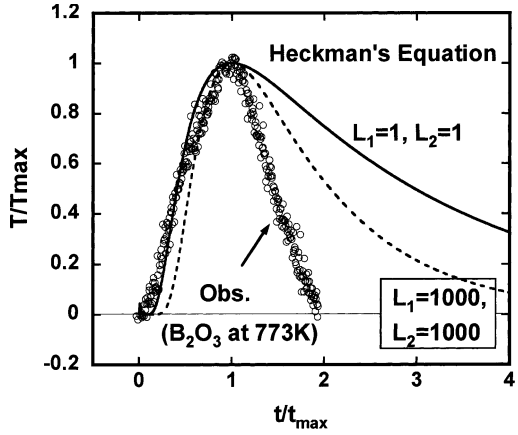

Fig. 7. Comparison of temperature profile between the observation and the calculation by Heckman's equation.

When the heat loss from the oxide sample surface by the radiation is taken into account (*e.g.*: $T_m=1\,000$ K, $D=0.001$ m, $\kappa=1$ W/m K), the order of L_m is less than one ($L_m \leqq 1$) in Eq. (9). As the heat loss in DHTT will be large at the detection thermocouple (CH-2) and the difference of heat loss between the radiation and the conduction is quite large, the characteristic two cases of heat loss are assumed as $L_1=L_2=1$ and $L_1=L_2=1\,000$ (triangular pulse; $\tau=0.2$ (pulse duration), $t_c=20.736$ and $b=0.1$: Appendix I).

In **Fig. 6**, the calculation results using Heckman's equation (Eq. (6)) under above two conditions are shown in comparison with Parker's equation (Eq. (2)). It was found that the existence of heat loss made the temperature profile lower and the local maximum point appeared on the temperature profile. Furthermore, the maximum point decreased with the increasing heat loss, intensely. It should be noted that the temperature profile never decrease in an insulated condition (Parker's equation, Eq. (2)) and the actual one must decreased more or less, because some extent of heat loss always exist.

These temperature profiles from Heckman's equation ($L_1=L_2=1$ and $L_1=L_2=1\,000$) were compared in **Fig. 7** with experimental data of B_2O_3 melt using DHTT at 773 K (the curves were normalized with T_{max} (the maximum tem-

perature) and t_{max} (the time at T_{max})). Even if the fairly large heat loss was assumed in the Heckman's equation ($L_1=L_2=1\,000$, broken line), the calculated temperature profile could not represent the experimental data, especially, the decreasing curve beyond the t_{max} did not represent the observation.

3.3. Numerical Method for DHTT Measurement

From above results, it was found that the analytical method was difficult to express the experimental results owing to the complex pulse shape and the heat loss in the present study. Then, the numerical analysis was carried out based on the following fundamental equation

$$\rho C_p \frac{\partial T}{\partial t}=\kappa \frac{\partial^2 T}{\partial x^2} \quad \text{.....(15)}$$

where ρ is the density, C_p is the heat capacity and κ is the thermal conductivity. The finite difference method with the forward differences was adopted for numerical analysis and the equation could be rewritten as follows[3]:

$$T_n^{i+1}=T_n^i+\alpha \frac{\Delta t}{\Delta x^2}(T_{n+1}^i-2T_n^i+T_{n+1}^i) \quad \text{.....(16)}$$

where 'n' means the position corresponding to the space-derivative and 'i' means the time corresponding to the time-derivative. The numerical calculation using Eq. (16) was carried out with $\Delta t=4\times10^{-6}$ (s) and $\Delta x=0.001$ (cm). The boundary condition at the front surface (heat source) was changed according to the experimental heat pulse.

$$T_0^i=f(t) \quad \text{.....(17)}$$

and the initial condition was

$$T_n^0=0 \quad \text{.....(18)}$$

Using Eq. (16), the temperature variation at the rear surface T_D^i (D means the position of rear surface) was calculated and compared with the analytical method (Eq. (2)), when the maximum temperature was kept at the rear surface for simulating the thermally insulated condition (without heat loss) and the instantaneous heat pulse was defined as $T_0^i=1$ in Eq. (17). The calculated results between the numerical method (Eq. (16)) and the analytical method (Eq. (2)) were shown in Fig. 4(b). It was confirmed that the present numerical method was in excellent agreement with the analytical method and was adequate to simulate the one dimensional heat transfer on the DHTT. The computer program was coded by Fortran 90 and the calculation time was 3 days on Pentium II, 1 hr on Pentium III and 10 min on Pentium IV. A large number of calculation with different conditions were performed.

Then, using experimental heat pulse (**Fig. 8**(a); the curve of pulse was divided into two region at the maximum point t_p ($0\leqq t\leqq t_p$ and $t>t_p$) and the two curves were expressed by the three dimensional polynomial), the numerical calculations were carried out and the temperature variations with different thermal diffusivities ($\alpha=0.001\times10^{-4}$–$0.005\times10^{-4}$ m^2/s) were compared with the observation in Fig. 8(b). It was found that the calculation result using the thermal diffusivity, $\alpha=0.003\times10^{-4}$ m^2/s was in good agreement with the observation. In this case, the heat pulse and the response curve were normalized by the t_p that was the time at the maximum temperature in the heat pulse.

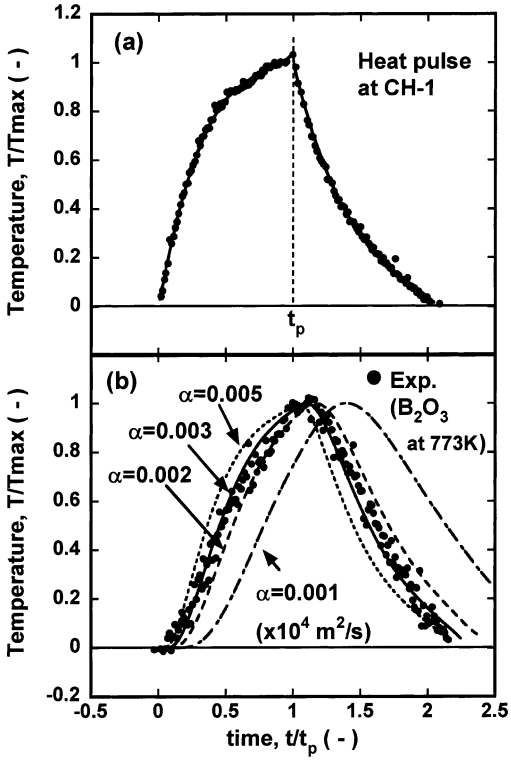

Fig. 8. Results of numerical analysis and comparison with the observation.

From these results, it could be concluded that not only the shape of pulse but also the heat loss affected the measurement of thermal diffusivity significantly in the DHTT measurement. The numerical method was useful to analyze the experimental heat response curve, because the shape of heat pulse was not geometric one and the heat loss from sample surface to both the ambient and the thermocouple was large. However, it is not practical method for getting a thermal diffusivity to use the numerical method owing to the necessity of huge work.

Then, the Eq. (4) will be convenient to obtain the thermal diffusivity. The parameters (ϑ_1 and ϑ_2) were determined as shown in the following section.

3.4. Parameters Determination (ϑ_1 and ϑ_2) for the Thermal Diffusivity on the DHTT Measurement

As mentioned above, the relationship between α and $t_{0.5}$ was obtained in the present study using the heat pulse simulating the experimental one with the numerical analysis. Before carrying out the numerical analysis, the relationships between α and $t_{0.5}$ in the Heckman's equation (Eq. (6)) were examined in the different conditions of heat loss. The results were shown in **Fig. 9**. The parameter ϑ_1 decreased with increasing heat loss ($L_1=L_2=1$ to $1\,000$) and the ϑ_2 increased slightly (the two lines seemed to be a parallel) with increasing heat loss. We have also calculated the line with $L_1=L_2=20$ and the result was almost the same as $L_1=L_2=1\,000$, which meant that the decrease from $L_1=L_2=20$ to $L_1=L_2=1\,000$ was very small.

Figure 10 shows the heat pulse functions for using the numerical analysis. The triangular pulse was also used for the comparison. The experimental pulse was formulated as

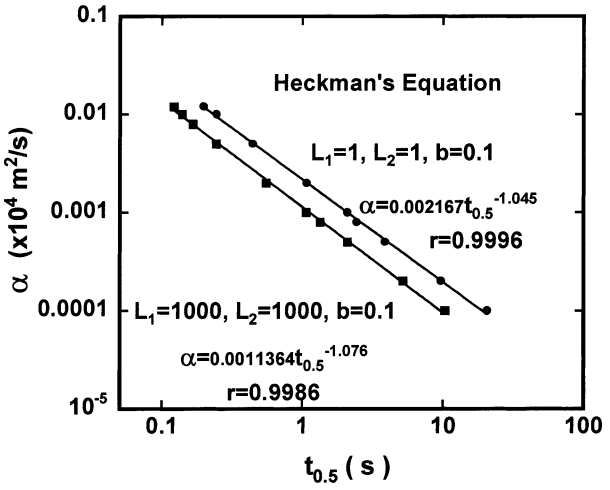

Fig. 9. Relationship between the thermal diffusivity α and the time at half-maximum temperature $t_{0.5}$ by Heckman's equitation.

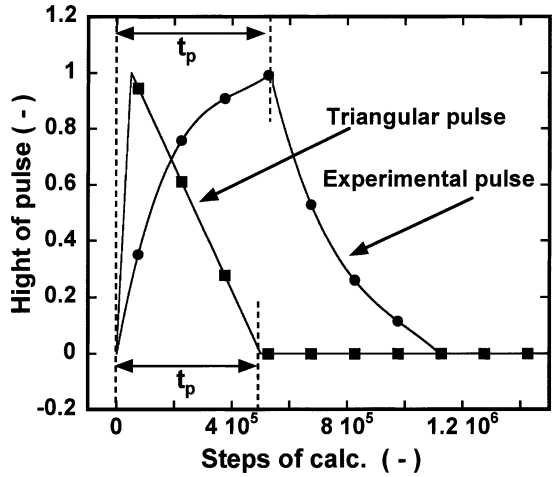

Fig. 10. Two types function of heat pulse used in the present numerical calculation.

the 3 dimensional polynomial (Fig. 8(a)) divided into two regions at t_p (maximum point). The definition of t_p was different between the experimental pulse and the triangular one, because the order of t_p in the triangular pulse was so small, if the maximum point was selected. On the other hand, in the experimental pulse, the decreasing curve from the maximum point depended on the condition of heat loss which was not constant between the different experiment. Sometime the period of decreasing curve was very long and difficult to define the period. Furthermore, there are some physical meaning for both the t_p. In the case of experimental pulse, t_p means the duration that the heating power is turning on, while the t_p in the triangular pulse means the duration that the laser pulse was changing into the heat at the front surface. From these reasons, the different definitions of t_p were selected as shown in Fig. 10.

Using two kind of heat pulses, the numerical method was carried out as mention above. The obtained results are shown in **Fig. 11**. The values of the parameter ϑ_1 in the both conditions were one order of magnitude smaller than that obtained using Heckman's equation (Fig. 9). The result was caused by the difference of the amount of heat loss. The numerical method could simulate the situation that the large

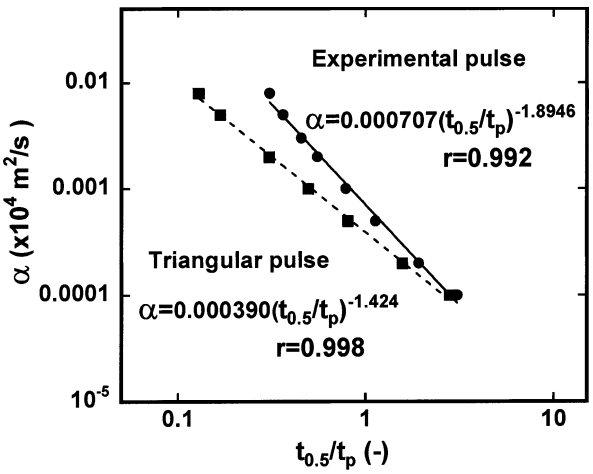

Fig. 11. Relationship between the thermal diffusivity α and the time at half-maximum temperature $t_{0.5}$ by the numerical method.

heat loss occurred in the DHTT. The parameter ϑ_2 was relatively larger than that of Heckman's. The relationship between α and $t_{0.5}$ obtained can be expressed as follows in the case of experimental heat pulse:

$$\alpha(\times 10^4\,\mathrm{m^2/s}) = 0.000707(t_{0.5}/t_p)^{-1.8946} \quad \text{.....(19)}$$

In the present experiment, $t_{0.5}/t_p$ was measured at the desired temperatures from 630 to 1 373 K using reagent grade B_2O_3 and also the thermal diffusivity α of B_2O_3 was calculated from the literature value (density ρ, the heat capacity C_p and thermal conductivity κ: Appendix II). These values were summarized in **Table 1** and shown in **Fig. 12**. Although some scattering can be seen in the observation, the variation with $t_{0.5}/t_p$ was in good agreement with the Eq. (19) that obtained by the numerical method. **Figure 13** shows the temperature dependence of thermal diffusivities obtained in the present study (using the observed $t_{0.5}/t_p$ and Eq. (19)) and the references value (Appendix II). The excellent agreement was obtained and the relationship between α and $t_{0.5}$ expressed by Eq. (19) was quite useful one to determine the thermal diffusivity using the DHTT.

However, another factor might govern the value obtained in high temperature range. That is a effect of radiation in a transparent sample[10–12] Moreover, this effect must dominant in both the data from the present study and the reference data (Appendix II, Ref. A8)), which was obtained by the steady-state method for thermal conductivity measurement, because both the thermal diffusivities increased with increasing temperature (normally, the thermal conductivity of glasses decreased in high temperature range[12]). This effect on the measurement of thermal diffusivity using DHTT will be discussed in the following paper.

Finally, the temperature response curves were calculated using the thermal diffusivity obtained by Eq. (19) and shown in **Fig. 14** ((a): 1 070 K, (b): 865 K). In these calculations, as each temperature profiles at heat source (at CH-1) were fitted to the three dimensional polynomial (as mentioned above, actually two kind of polynomials used for two regions before and after the maximum temperature) and used in the numerical calculation, it is natural that the circles (observations) and the lines (calculation) in Figs. 14(a) and 14(b) were almost the same line. On the other hand, the

Table 1. Thermal diffusivity obtained in present study.

Temperature K	$t_{0.5}$/tp	α calc. (APPENDIX II)	α Present work (Eq.(19))
633	0.40278	0.0046400	0.0039597
746	0.39167	0.0043000	0.0041752
778	0.35086	0.0044850	0.0051429
828	0.37500	0.0048000	0.0045338
866	0.37500	0.0050400	0.0045338
921	0.30830	0.0053900	0.0065707
982	0.30830	0.0055000	0.0065707
1018	0.32080	0.0059500	0.0060941
1066	0.30110	0.0063200	0.0068715
1111	0.29417	0.0066100	0.0071815
1164	0.29000	0.0067800	0.0073784
1229	0.24560	0.0081800	0.010109
1290	0.25000	0.0094900	0.0097742
1373	0.23216	0.011400	0.011246

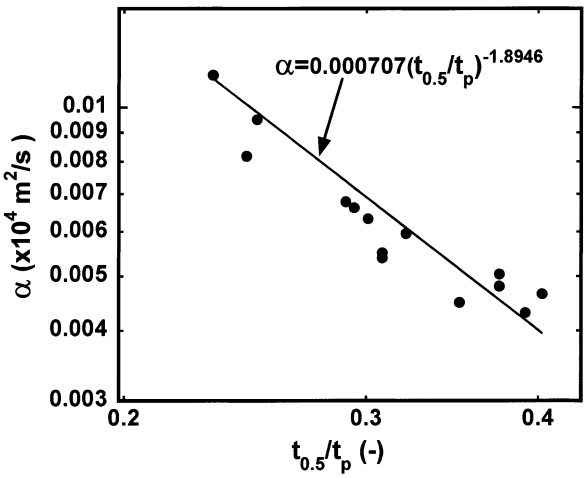

Fig. 12. Relationship between thermal diffusivity α and $t_{0.5}/t_p$.

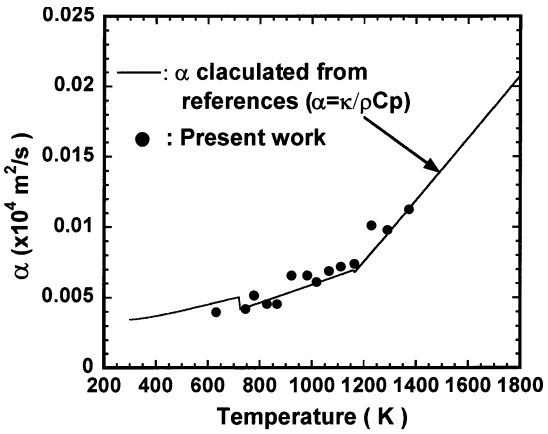

Fig. 13. Comparison of thermal diffusivity between the observation and the literatures.

temperature profiles at the rear surface (at CH-2) were shown in squares and lines. There were excellent agreement between the calculations and observations at both the temperatures.

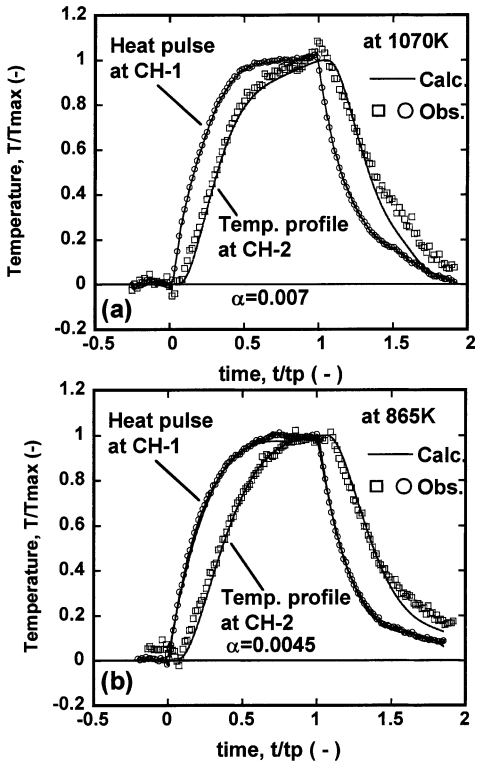

Fig. 14. Comparison of temperature profiles between the calculation and observation using the thermal diffusivity obtained by Eq. (19).

4. Conclusions

New method to measure the thermal diffusivity using double hot thermocouple technique (DHTT) was developed. The factors affecting on the thermal diffusivity measurement were elucidated. The finite pulse-time effect and the heat loss were quite different from that of laser pulse method and it was found that the analytical method could not used for the DHTT. Then, numerical method was applied to analyze the heat conduction on the DHTT.

The results obtained are as follows:

(1) The heat loss in DHTT was quite high and the analytical method presented by Heckman could not apply.

(2) In addition , since the shape and duration of pulse

in the heat source was entirely different from the laser flash method, the numerical method was useful to simulated the heat transfer on the DHTT.

(3) The new relationship between the thermal diffusivity α and the time at the half-maximum temperature $t_{0.5}$ was obtained using the numerical method, which was in excellent agreement with the observation.

$$\alpha(\times 10^4\,\mathrm{m^2/s}) = 0.000707(t_{0.5}/t_p)^{-1.8946}$$

Acknowledgment

A part of this project was performed with the support of the ISIJ Research Promotion Grant from 1999 to 2001. The authors would like to express the deep appreciation to the ISIJ and the persons who concerned.

REFERENCES

1) Y. Kashiwaya, C. E. Cicutti, A. W. Cramb and K. Ishii: *ISIJ Int.*, **38** (1998), 348.
2) Y. Kashiwaya, C. E. Cicutti and A. W. Cramb: *ISIJ Int.*, **38** (1998), 357.
3) H. S. Carslaw and J. C. Jaeger: Conduction of Heat Transfer in Solids, 2nd ed., Oxford University Press, New York, (1959), 101.
4) W. J. Parker, R. J. Jenkins, C. P. Butler and G. L. Abbott: *J. Appl. Phys.*, **32** (1961), 1679.
5) K. B. Larson and K. Koyama: *J. Appl. Phys.*, **38** (1967), 465.
6) R. E. Taylor and J. A. Cape, *Appl. Phys. Lett.*, **5** (1964), 212.
7) J. A. Cape and G. W. Lehman: *J. Appl. Phys.*, **34** (1963), 1909.
8) D. A. Watt: *Brit. J. Appl. Phys.*, **17** (1966), 231.
9) R. C. Heckman: *J. Appl. Phys.*, **44** (1973), 1455.
10) R. Gardon: *J. Am. Ceram. Soc.*, **44** (1961), 305.
11) W. D. Kingery: *J. Am. Ceram. Soc.*, **44** (1961), 302.
12) K. Nagata, M. Susa and K. Goto: *Tetsu-to-Hagané*, **69** (1983), 1417.

Table A1. Numerical solutions of Eq. (7).

β_n	L_1=1, L_2=1	L_1=1000, L_2=1000
β_1=	1.306542374193668	3.135322030076839
β_2=	3.673194406554103	6.270644183187904
β_3=	6.584620042704046	9.405966582352988
β_4=	9.631684635765851	12.54128935056289
β_5=	12.72324078413658	15.67661261076511
β_6=	15.83410536934389	18.81193648584928
β_7=	18.95497141085798	21.94726109863283
β_8=	22.08165963593638	25.08258657184653
β_9=	25.21202688856283	28.21791302812015
β_{10}=	28.34486414960702	31.3532405899681
β_{11}=	31.4794387120055	34.48856937977514
β_{12}=	34.61528107483173	37.62389951978204
β_{13}=	37.75207667597715	40.75923113207145
β_{14}=	40.88960693324043	43.89456433855361

Appendix I

Table A1 shows the numerical solution for the positive root of Eq. (7) (calculated by double precision, error is less than 10^{-12}) (usually, $n<13$ was enough for the precise calculation.)

$$(\beta_n^2 - L_1L_2)\tan\beta_n = \beta_n(L_1+L_2)$$

Appendix II

The thermal diffusivity of B_2O_3 was calculated using the data listed in **Table A2**. Although the density from the liter-

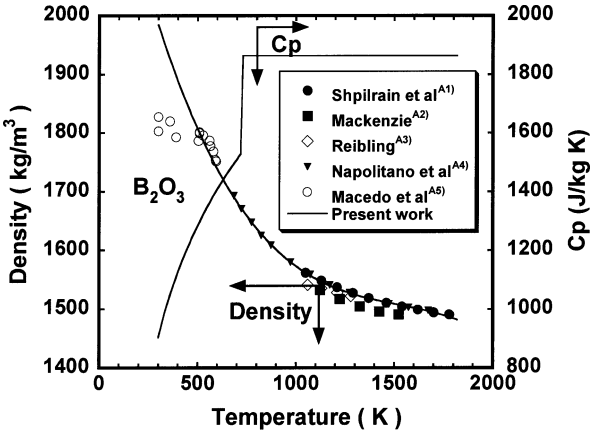

Fig. A1. Density and heat capacity of B_2O_3 from literatures.

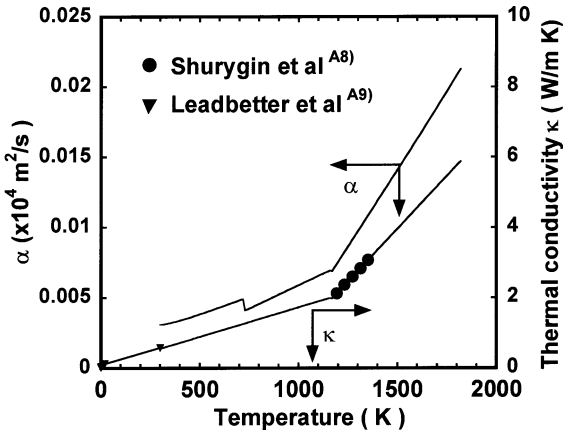

Fig. A2. Thermal conductivity and diffusivity from literatures.

Table A2. References data on B_2O_3 for calculating the thermal diffusivity.

	Equations for the thermochemical properties based on the references	Temperature Range	References
Density ρ (kg/m^3)	$2373.4 - 1.5734T + 0.00098982T^2 - 2.1674\times10^{-7}T^3$	300-1800K	A1 – A5)
Heat capacity Cp(J/kg K)	$[48.277-2\times(-57.728\times10^{-3})T-2\times(0.706\times10^{6})T^{-2}-6\times(7.054\times10^{-6})T^2-(37.749/4)T^{-0.5}]\times1000/69.622$	289 – 723K	A6,A7)
	1863.02	> 723K	A6,A7)
Thermal conductivity κ (W/m K)	0.054535+0.0016727T	0K-1173K	A8,A9)
	-5.04+0.006T	1173K-1373K	

atures has some scattering, the data from Shpilrain *et al*.[A1] and Napolitano *et al*.[A4] shows a good agreement. The regression curve for density has made based on their data (**Fig. A1**). There is a few data on the heat capacity of B_2O_3,[A6,A7] the sudden increase at 723 K corresponds to the transformation (Fig. A1). **Figure A2** shows the variation of the thermal conductivity of B_2O_3, the data is also a few and only two regions can be available (from 0 to 300 K and from 1 173 to 1 373 K).[A8,A9] In present study, two lines were used for expressing the two regions. Then, thermal diffusivity was estimated using these data ($\alpha = \kappa/(\rho C_p)$) and shown in Fig. A2.

A1) E. E. Shpilrain, K. A.Yakimovich and A. F. Tsitsarkin: *Teplofiz. Vys. Temp*., **9** (1971), 67.
A2) J. D. Mackenzie: *J. Phys. Chem*., **63** (1959), 1875.
A3) E. F. Riebling: *J. Am. Ceram. Soc.*, **47** (1964), 478.
A4) A. Napolitano, P B. Macedo and E. G. Hawkins: *J. Am. Ceram. Soc.*, **48** (1965), 613.
A5) P. B. Macedo, W. Capps and T. A. Litovitz: *J. Chem. Phys.*, **44** (1966), 3357.
A6) K. Fajams and S. W. Barber: *J. Am. Chem. Soc.*, **74** (1952), 2761.
A7) M. Chase et al.: JANAF Thermochemical Tables, 3rd ed., J. Phys. Chem. Ref. Data, (1985).
A8) P. M. Shurygin, V. P. Buzovkin and V. V. Leonov: *Teplofiz. Vys. Temp.*, **14** (1976), 1101.
A9) A. J. Leadbetter, A. P. Jeapes, C. G. Waterfield and R. Maynard: *J. Phys.* (*Paris*), **38** (1977), 95.